Off-shell effect in Rydberg-atom–alkali-metal-atom scattering

Dimitri B. Khrebtukov and Ilya I. Fabrikant
Department of Physics and Astronomy, University of Nebraska, Lincoln, Nebraska 68588-0111
(Received 16 January 1995)

We study the Rydberg-atom–ground-state-atom collisions within the framework of the quasi-free-electron model. We show that the general formulation of the problem based on the three-body Faddeev equations requires the off-shell extension of the two-body amplitude for electron-atom scattering. The two-body off-shell amplitudes for electron scattering by Rb and Cs atoms are calculated using the pseudopotential approach. The cross section for collisional quenching and broadening of Rydberg states due to perturbations by Rb and Cs atoms are calculated, and the results are compared with experimental data. The off-shell extension of the scattering amplitude usually improves agreement with the experiment. However, both on-shell and off-shell results fail in the region of low principal quantum numbers, where the multiscattering effects become important. Our calculations and their comparison with the experiments confirm that the $Cs^-(^3P)$ state is a resonance rather than a bound state.

PACS number(s): 34.60.+z, 32.70.Jz

I. INTRODUCTION

Collisions of highly excited Rydberg atoms (A^{**}) with ground-state atoms (B) represent a typical three-body problem of quantum mechanics. In contrast to a more common case of the Coulomb interaction between all particles, we have here the Coulomb interaction between one pair of particles (Rydberg electron e and the ion core A^+) and short-range interactions between two other pairs (e-B and A^+-B). There are two different approaches to the theoretical investigation of this problem: the quasi-free-electron model [1], or impulse approximation [2], and the adiabatic quasimolecular approach [3]. The quasi-free-electron model is more justified for a high principal quantum number n of the Rydberg atom. In this case the Rydberg electron interacts only once with the perturber B during the collision. However, for lower n the A^{**}-B collision cannot be considered as e-B or A^+-B scattering event any longer. The multiscattering effects can be neglected if [4] (atomic units are used throughout the paper)

$$v_{AB} > \frac{r_{e\text{-}B}}{2\pi n^3}, \tag{1}$$

where v_{AB} is the relative velocity of the colliding partners and $r_{e\text{-}B}$ is the effective radius of the e-B interaction. There are other conditions for the impulse approximation to be valid, discussed in the literature [2,5,6], but the condition (1) imposes the strongest restriction on n for thermal collisions with a typical collision velocity of 2×10^{-4} a.u. This especially concerns collisions with alkali-metal atoms, where the radius $r_{e\text{-}B}$, is very large due to both a large polarizability of the perturber B and a low-energy ^3P resonance in e-B scattering. In this case the typical limit on n given by (1) is $n > 25$.

On the other hand, the adiabatic quasimolecular approach can be applied for low enough n, when the number of coupled equations to be solved is reasonably small. Borodin and Kazansky [7] suggested a special method to incorporate the low-energy ^3P resonance within the framework of the adiabatic approximation. This allowed us [4,8] to describe the experimentally observed [9,10] oscillatory n dependence of the Rydberg state broadening due to collisions with the ground-state alkali-metal atoms. However, this model does not give a smooth transition to the impulse-approximation limit at high n [8].

An approach permitting the complete description of the three-body dynamics and allowing, in principle, the smooth transition from low-n to high-n limit is that of three-body Faddeev equations [11]. This method is actually more suited to solution of three-body problem with two short-range interactions rather than to the three-body Coulomb problem because the latter experiences substantial difficulties with convergence [12]. Recently we showed [6] how to set up the Faddeev equations for the problem of A^{**}-B collisions and how these equations can be reduced to the conventional impulse approximation. The important step in this procedure is the on-shell reduction of the two-body scattering operator describing e-B collisions. This reduction can be justified for the case of a rare-gas-atom as a perturber [13]. In this case the e-B scattering operator can be given with a good accuracy by the scattering-length approximation and does not depend strongly on the energy. However, the case of an alkali-metal perturber is quite different. The scattering-length approximation becomes valid only for very low energies (below about 1 meV); therefore for $n < 100$ we should generally use the off-shell amplitude. The main purpose of this paper is to study the off-shell effects in collisions of Rydberg atoms with ground-state–alkali-metal atoms. We will do it in the first approximation of the Faddeev theory, which is similar to the impulse approximation, but includes the off-shell two-body amplitude. In the next section we derive the first-order Faddeev approximation, in Secs. III and IV we discuss the method of calculation of the off-shell scattering amplitudes, and in Sec. V we present our results on collisional cross sec-

tions and broadening rates and their comparison with experimental data.

II. FIRST-ORDER FADDEEV APPROXIMATION

In order to show how the off-shell effects appear in the quasi-free-electron model we consider the Faddeev equations describing Rydberg-atom–ground-state-atom scattering. They were written and employed before in Refs. [6,14] and only a brief outline will be given here.

Let us consider the Rydberg atom A as a system consisting of particles 1 (the ion core A^+) and 2 (the Rydberg electron). This system interacts with a particle 3 (the perturber B). We introduce the Jacobi momentum coordinates

$$\mathbf{k}_{21} = \frac{m_1\mathbf{k}_2 - m_2\mathbf{k}_1}{m_1+m_2}, \qquad \mathbf{q}_3 = \frac{(m_1+m_2)\mathbf{k}_3 - m_3(\mathbf{k}_1+\mathbf{k}_2)}{m_1+m_2+m_3}. \tag{2}$$

The alternative Jacobi coordinates could be obtained by an appropriate interchange of indices.

Introducing the two-particle Faddeev operators T_{ij} and $T^{(ij)}$ [11], we have the set of equations

$$T^{(12)} = \tilde{T}_{12} - T_{12}G_0(T^{(13)} + T^{(23)}), \tag{3}$$

$$T^{(13)} = -T_{13}G_0(T^{(12)} + T^{(23)}), \tag{4}$$

$$T^{(23)} = -T_{23}G_0(T^{(12)} + T^{(13)}), \tag{5}$$

where G_0 is the three-body Green's function for noninteracting particles and $\tilde{T}_{12}$ describes the initial bound state of A^+ and e and has the form

$$\tilde{T}_{12}(\mathbf{k}_{21},\mathbf{q}_3) = -\delta(\mathbf{q}_3-\mathbf{p})\left(\mid \epsilon_i \mid + \frac{k_{21}^2}{2m_{12}}\right)\phi_{\epsilon_i}(\mathbf{k}_{21}), \tag{6}$$

where $\mathbf{p}$ is the initial momentum of B relative to A, ϵ_i is the energy of the bound state, m_{12} is the reduced mass (in our case $m_{12}\approx m_2$), and $\phi_{\epsilon_i}(\mathbf{k}_{21})$ is the initial bound-state wave function in the momentum space. T_{13} has the form

$$T_{13}(\mathbf{k}'_{31},\mathbf{q}'_2;\mathbf{k}_{31},\mathbf{q}_2;E) = t_{13}(\mathbf{k}'_{31},\mathbf{k}_{31};\epsilon_2)\delta(\mathbf{q}'_2-\mathbf{q}_2), \tag{7}$$

where

$$\epsilon_2 = E - \frac{q_2^2}{2\mu_2}, \qquad \mu_2 = \frac{m_2(m_1+m_3)}{m_1+m_2+m_3}, \tag{8}$$

t_{13} is the t operator for the two-body problem, and E is the total energy. T_{12} and T_{23} are defined in a similar way.

Equations (3)–(5) should be solved for $T^{(12)}, T^{(13)}, T^{(23)}$. Then the cross section for B-A scattering, accompanied by the transition $f \leftarrow i$ in the target, is

$$d\sigma_{f\leftarrow i} = \frac{p'}{p}(m_{13})^2(2\pi)^4 d\hat{p}' \mid \mathcal{T}^{(1)}_{f\leftarrow i} + \mathcal{T}^{(2)}_{f\leftarrow i} \mid^2, \tag{9}$$

$$\mathcal{T}^{(n)}_{f\leftarrow i} = -\int \Phi^*_f(\mathbf{k}_{21},\mathbf{q}_3)T^{(n3)}(\mathbf{k}_{21},\mathbf{q}_3)d\mathbf{k}_{21}d\mathbf{q}_3, \tag{10}$$

where

$$\Phi_f(\mathbf{k}_{21},\mathbf{q}_3) = \phi_{\epsilon_f}(\mathbf{k}_{21})\delta(\mathbf{q}_3-\mathbf{p}') \tag{11}$$

is the final-state wave function, $\mathbf{p}'$ being the relative momentum in the final state.

The first-order Faddeev approximation can be obtained from Eqs. (3)–(5) by setting $T_{12} = T_{13} = 0$. This means that during the scattering process the ion core does not interact with both the Rydberg electron and the perturber. In fact, the ion-core–perturber polarization interaction is important in elastic scattering. However, as we have shown before [6], the contribution of this interaction to the scattering cross section may be considered independently, since the simultaneous electron-perturber and ion-perturber interactions are unlikely. Let us concentrate here on the electron-perturber contribution. Employing the smallness of the electron mass as compared to the masses of the ion core and the perturber, and assuming that the relative A-B momentum is much greater than the electron momentum and the relative collision velocity is much smaller than the electron's velocity (the typical conditions for the thermal-energy collisions), we obtain for the electron-perturber contribution to the scattering amplitude

$$\mathcal{T}^{(2)}_{f\leftarrow i} = -\int \phi^*_{\epsilon_f}(\mathbf{k}_{21}+\mathbf{Q})t_{23}\left(\mathbf{k}_{21}+\mathbf{Q},\mathbf{k}_{21};E-\frac{p^2}{2\mu_1}\right) \times \phi_{\epsilon_i}(\mathbf{k}_{21})d\mathbf{k}_{21}, \tag{12}$$

where $\mathbf{Q} = \mathbf{p} - \mathbf{p}'$ is the momentum transfer.

Equation (11) represents the first-order Faddeev approximation. It can be reduced to the standard impulse approximation if we use the on-shell reduction of the two-body t operator. However, if the energy and momentum dependence of the off-shell scattering amplitude is strong, this reduction can change the results substantially. In particular, a big difference can occur in the case of a low-energy narrow resonance in the free-electron–atom scattering. In this case the on-shell scattering amplitude as a function of momentum has a sharp peak and according to Matsuzawa [15] this causes oscillations in dependence of collisional or broadening cross sections as functions of the principal quantum number of the Rydberg atom. However, if one uses the off-shell scattering amplitude, no oscillations occur since the scattering amplitude as a function of the electron momentum does not have a peak at negative energies. The second type of behavior of the scattering cross sections seems to be more reasonable because it provides a smooth transition from the case of a low-energy resonance to the case of a bound state. Regarding the experimentally observed oscillations [9,10] in the n dependence of the Rydberg-state broadening due to collisions with alkali-metal atoms, it was shown [16] that the Matsuzawa's mechanism cannot describe quantitatively these oscillations and another mechanism was suggested [7], which involves multiple-scattering approach.

Another case that indicates a substantial difference between the impulse and the first-order Faddeev approximations involves the existence of a weakly bound state of electron in the perturber's field. The on-shell scattering amplitude does not contain any singularity for a real mo-

mentum, although it has a peak in the case of the s-wave scattering. The off-shell scattering amplitude does have a pole at negative energy corresponding to that of the bound state. The position of this pole does not depend on the momentum and causes a very strong increase of the scattering cross section as the binding energy of the electron in the Rydberg atom approaches the binding energy of the negative ion B^-. (Of course, the first-order approximation becomes invalid in this case.) In particular, a bound state of p symmetry does not affect the broadening cross section calculated in the impulse approximation [6], but does affect the cross section calculated in the first-order Faddeev approximation. Once again, the second type of behavior seems to be more physical.

Equation (11) can be used to calculate the collisional shift and broadening of Rydberg states. If the scattering amplitude is exact, the shift and the width are determined by the real and the imaginary part of the amplitude respectively. Alekseev and Sobel'man [17] suggested the use of this relation employing the scattering amplitude calculated in the impulse approximation. However, the determination of the width in terms of the imaginary part of the scattering amplitude implies the validity of the optical theorem and the latter is violated in the impulse approximation [2]. This can lead to unphysical results. In particular, the level's width does not disappear in the limit of small relative velocities when the energy of the system Rydberg atom plus the perturber cannot have an imaginary part. Omont [18] showed that the equation of Alekseev and Sobel'man is valid in the limit $n^2 \gg v_{AB}^{-1}$. For thermal velocities this condition typically implies n values at least greater than 70.

Lebedev and Marchenko [19] suggested another approach, employing the impulse approximation but not using the optical theorem. Recently we showed [6] that their equation for the inelastic (quenching) cross section describes satisfactorily experimental data on Rb(nS)-Rb collisions. We can incorporate the first-order Faddeev approximation into this equation and check how the off-shell extension of the scattering amplitude affects the cross section. The derivation of the equation for the quenching cross section is very similar to that given in Ref. [19] and we will present here only the final result:

$$\sigma_{nl}^{\text{inel}} = \frac{\pi}{v_{AB}^2} \sum_{n'} \frac{1}{(n')^3} \int_{Q_{\min}}^{Q_{\max}} dQ \int_{|k_0(Q)|}^{\infty} k dk g_{nl}(k) \mid^2 \times \mid f_{eB}(k, k', \cos\theta', \epsilon_i) \mid^2, \tag{13}$$

where $Q_{\min} = \mid \Delta\epsilon \mid / v_{AB}$, $\Delta\epsilon$ being the energy defect for the inelastic transition, $Q_{\max} = 2\mu v_{AB}$, where μ is the reduced mass of the A-B system, and g_{nl} is the radial part of the electron wave function in the momentum space. The lower limit of integration over k is given by

$$k_0(Q) = \frac{Q}{2} - \frac{\Delta\epsilon}{Q}.$$

The off-shell e-B scattering amplitude f_{eB} is considered as a function of four variables: the initial momentum k, the final momentum k', the angle θ' between $\mathbf{k}$ and $\mathbf{k}'$, and the electron energy ϵ_i. In Eq. (12) these variables are connected by the equations

$$(k')^2 = k^2 + 2\Delta\epsilon, \tag{14}$$

$$\cos\theta' = \frac{k^2 + \Delta\epsilon - Q^2/2}{kk'}. \tag{15}$$

These equations represent conservation of energy and momentum in the A-B collisions.

There are two modifications in Eq. (13) compared to that of Lebedev and Marchenko. First, the absolute values of momenta k and k' in Eq. (13) are not identical. This modification is not important, since a typical kinetic energy of the Rydberg electron equals $1/n^2$, whereas a typical energy transfer determining the difference between k and k' is less than $1/n^3$. The second modification, the negative value of ϵ_i in Eq. (13), is much more substantial. We will analyze it below considering the Rb and Cs atoms as examples.

III. CALCULATION OF THE OFF-SHELL SCATTERING OPERATOR

In Refs. [6,16] the on-shell amplitude for low-energy electron scattering by alkali-metal atoms was studied. To extend this amplitude off the energy shell a complete information on the electron-atom interaction is necessary. In principle, knowing the on-shell scattering phase shifts and the negative-ion binding energies one can reconstruct the scattering potential [20]. In the case of the electron-atom interaction the situation is complicated by the Pauli exclusion principle. The actual electron-atom interaction includes a nonlocal exchange operator. However, at low enough energies this effect can be incorporated by introducing the pseudopotential [21]

$$V = \sum_{S,l,m} \frac{2l+1}{4\pi} \mid Y_{lm}(\hat{r}')\rangle v_l^S \langle Y_{lm}(\hat{r}) \mid . \tag{16}$$

This equation simply suggests that for each combination of the electron orbital angular momentum l and the total spin S of the e-B system there is a spherically symmetric potential v_l^S describing the e-B scattering. Assuming that only two partial waves (s and p) contribute nontrivially to the scattering amplitude, we have to find four spherically symmetric potentials corresponding to ^1S, ^3S, ^1P, and ^3P scattering. The higher partial waves for low-energy scattering can be described in terms of the Born phase shifts [16].

The scattering t operator satisfies the Lippman-Schwinger equation [22]

$$t(E) = v - v g^{(0)}(E) t(E), \tag{17}$$

where $g^{(0)}(E)$ is the Green's function for the free motion

$$g^{(0)}(E) = [H_0 - (E + i\eta)]^{-1}, \quad \eta \to 0.$$

The solution of Eq. (17) can be expressed in terms of the Green's function of the full Hamiltonian [22]

$$t(E) = v - vg(E)v, \tag{18}$$

$$g(E) = [H_0 + v - (E + i\eta)]^{-1}.$$

Using the momentum representation for t and expanding $t(E)$ and $g(E)$ in partial waves

$$t(E) = \sum_l (2l+1) t_l(k', k, E) P_l(\cos\theta), \tag{19}$$

$$g(\mathbf{r}, \mathbf{r}', E) = \sum_{l,m} g_l(r, r', E) Y_{lm}(\hat{r}) Y^*_{lm}(\hat{r}'), \tag{20}$$

where θ is the scattering angle, and using Eq. (18), we obtain

$$t_l(k', k, E) = t_l^{(1)}(k', k) + t_l^{(2)}(k', k, E), \tag{21}$$

$$t_l^{(1)}(k', k) = \frac{1}{2\pi^2} \int j_l(k'r) v_l(r) j_l(kr) r^2 dr, \tag{22}$$

$$t_l^{(2)}(k', k, E) = -\frac{1}{2\pi^2} \int j_l(k'r') v_l(r') g_l(r', r, E) \times v_l(r) j_l(kr) (r')^2 r^2 dr' dr, \tag{23}$$

where j_l is the spherical Bessel function. For numerical calculations it is convenient to introduce the function

$$u_l(r', k, E) = -\frac{r'}{2} \int g_l(r', r, E) v_l(r) j_l(kr) r^2 dr, \tag{24}$$

which satisfies the differential equation

$$\left[\frac{d^2}{dr^2} - \frac{l(l+1)}{r^2} + 2E - 2v_l(r)\right] u_l(r) = r j_l(kr) v_l(r). \tag{25}$$

The boundary conditions depend on the sign of energy. For positive energies $E > 0$ we can specify the outgoing-wave boundary conditions to guarantee the correct on-shell result, i.e.,

$$u_l(r) \to C(E) \exp(i\sqrt{2E} r) \text{ as } r \to \infty \ (E > 0), \tag{26}$$

where $C(E)$ is defined uniquely by the differential equation (25).

However, for $E < 0$ the right-hand side of Eq. (25) prevails over the decaying exponential in Eq. (26) and the boundary condition depends on the asymptotic behavior of the potential $v_l(r)$. In our case the potential at large distances is $v_l(r) \approx -\alpha/(2r^4)$ [see Eq. (29) below], where α is the polarizability of the atomic perturber. The boundary condition for negative energies becomes

$$u_l(r) \to \frac{\alpha}{2r^4} \frac{1}{k^2 + 2|E|} \left(r j_l(kr) - \frac{8k}{k^2 + 2|E|} j_{l-1}(kr) \right) + O\left(\frac{1}{r^6}\right) \text{ as } r \to \infty \ (E < 0). \tag{27}$$

Equation (25) can be integrated numerically and the second contribution to the t operator is given by

$$t_l^{(2)}(k', k, E) = \frac{1}{\pi^2} \int r j_l(k'r) v_l(r) u_l(r, k, E) dr. \tag{28}$$

The off-shell scattering amplitude differs only by a numerical coefficient from the scattering operator (in atomic units)

$$f(E) = -4\pi^2 t(E).$$

IV. CALCULATION OF THE PSEUDOPOTENTIAL

The problem has been reduced to construction of spherically symmetric potentials $v_l^S(r)$. We have done this by parametrizing the function $v_l^S(r)$ in the form

$$v(r) = -\frac{1}{r} \frac{\sum_{j=1}^{N} a_j r^{(j-1)}}{\sum_{j=1}^{N} b_j r^{(j-1)}} \sum_{j=1}^{M} c_j \exp(-r/s_j) - \frac{\alpha}{2} \{1 + (d_1^2 - 1) \exp[-d_2(r - r_0)]\} \times \left(\frac{1 - \exp(-r/d_3)}{r} \right)^4, \tag{29}$$

where α is the polarizability, r_0 is the radius of the hard core to take into account the Pauli exclusion principle (see the discussion below), and the coefficients a_j, b_j, c_j, s_j, and d_j are fit parameters that should reproduce the low-energy scattering phase shifts and the energy of the bound negative-ion ^1S state. Although this problem can be solved in principal on the whole real-energy axis [20], for our applications only the low-energy region is important; therefore the potentials obtained in this work reproduce the scattering features only in the region below about 1 eV.

Since we do not include explicitly the exchange interaction, our pseudopotential should take care of the Pauli exclusion principle. In particular, it should be repulsive at short distances to avoid an appearance of the bound states associated with the inner-shell electrons. Our calculations have shown that this repulsion is very strong and corresponds practically to an infinite wall at r between 3.6 and 5.2 a.u. Although this does not cause a problem in the fit procedure, this leads to divergencies for $t^{(1)}$ and $t^{(2)}$ in Eqs. (22) and (23). In fact, these divergencies compensate each other and the final result for t is finite. To analyze the behavior of the scattering operator in this case we have considered scattering by a potential with a hard core. All necessary equations for this case are given in Appendixes A and B.

For our fit procedure we used the Nelder-Meade simplex algorithm [23] to minimize the sum of the absolute differences between the phase shifts calculated with the potential given by Eq. (29) and the phase shifts obtained by the modified effective range theory [16,24,25]. To en-

TABLE I. Parameters of the potentials.

Potential	α	r_0	N	a_j	b_j	M	c_j	s_j	$d_{\{1,2,3\}}$
Rb ^1S	328	4.04	3	61278091	137699.41	2	91.389989	0.57981914	1.7396640
				-22229927	155428.21		161.63356	0.40456942	0.14976577
				6615418.3	49379.489				4.3738002
Rb ^3S	328	5.0	1	-126.03096	53.466903	1	13.766280	2.2646836	1.8734923
									0.16545671
									0.26222017
Rb ^1P	328	2.8	2	-239.60267	0.0028933263	2	-2.0048060	0.32744923	0.034193255
				-0.46375238	0.0010664387		0.14898776	0.18509251	0.17694527
									5.9889732
Rb ^3P	328	3.878	3	46083384	-6175.5154	2	62.916566	0.61059330	1.0311556
				-27057553	-1127.4859		477.18992	0.26963274	0.0055405060
				5033759.8	24040.626				3.7912937
Cs ^1S	402	3.878	3	37040856	177877.57	2	86.887285	0.59902520	1.3841794
				-20399750	110012.28		171.60150	0.45744529	0.12667271
				5848821.0	49124.547				4.6774974
Cs ^3S	402	5.0	1	-49.810816	20.964605	1	9.1911958	2.1857269	1.3414170
									14.979380
									2.9865104
Cs ^1P	402	3.9	1	-19.941913	11.367579	1	24.623086	1.5416545	0.89139250
									0.24999025
									4.6409640
Cs ^3P	402	3.878	3	36168743	-6070.6198	2	54.513680	0.60432915	1.0349518
(resonance)				-28988912	-1102.3471		471.47533	0.26561496	0.0048422922
				6650590.8	24457.553				4.8255784
Cs ^3P	402	3.878	3	25717702	594.94084	2	57.029834	0.62844539	1.1931197
(bound				-24141361	1017.9819		15.516507	0.029868476	0.11465591
state)				4900896.9	34556.585				3.7909393

sure the proper negative ion bound state energy values, the radial Schrödinger equation with the potential (29) has been integrated twice—from the hard core with zero boundary condition on the core and from the infinity with exponential decay boundary condition—and the absolute difference of the logarithmic derivatives was added to the sum of the phase shift differences.

The results of our fit procedure are presented in Table I. The ^1S potential exhibits a deep and narrow minimum at $r = 5.6$ a.u., supporting one bound state with binding energy 0.486 eV for Rb and 0.471 for Cs. The ^3S potential has a very shallow minimum at large distances of about 13 a.u., supporting a virtual state. The latter leads to the large in absolute magnitude ^3S scattering length $A = -16.9$ a.u. for Rb and $A = -22.7$ a.u. for Cs [16]. The ^3P potential (including the centrifugal part) has a deep and narrow minimum at $r = 3.6$ a.u., and a low barrier at $r = 17$ a.u., providing a low-energy resonance with the position $\epsilon = 0.023$ eV and width $\Gamma = 0.025$ eV [16] for Rb and $\epsilon = 0.0126$ eV and $\Gamma = 0.0091$ eV for Cs.

V. RESULTS AND DISCUSSION

In Figs. 1 and 2 we present the k dependence of the off-shell amplitude $f(k, k, E)$ for different negative values of the energy E. They are related to the principal quantum number n by the Rydberg formula $E = -1/2(n-\mu)^2$ and for the quantum defect we have chosen $\mu = 3.133$ and $\mu = 4.049$ for Rb and Cs, respectively. They correspond to the nS levels. At high n the off-shell amplitude is close to the real part of the on-shell amplitude; therefore we do not expect any drastic changes in the Rydberg collision cross sections in this region. However, for lower n the difference is very large. In particular, when E approaches the energy of the ^1S bound state, corresponding to $n - \mu = 5.29$, the off-shell amplitude diverges. On the other hand, for such low n both the impulse and the first-order Faddeev approximation are very unlikely to be valid.

Very striking changes occur in the ^3P scattering. The off-shell amplitude as a function of momentum no longer exhibits the resonance behavior since it behaves in the

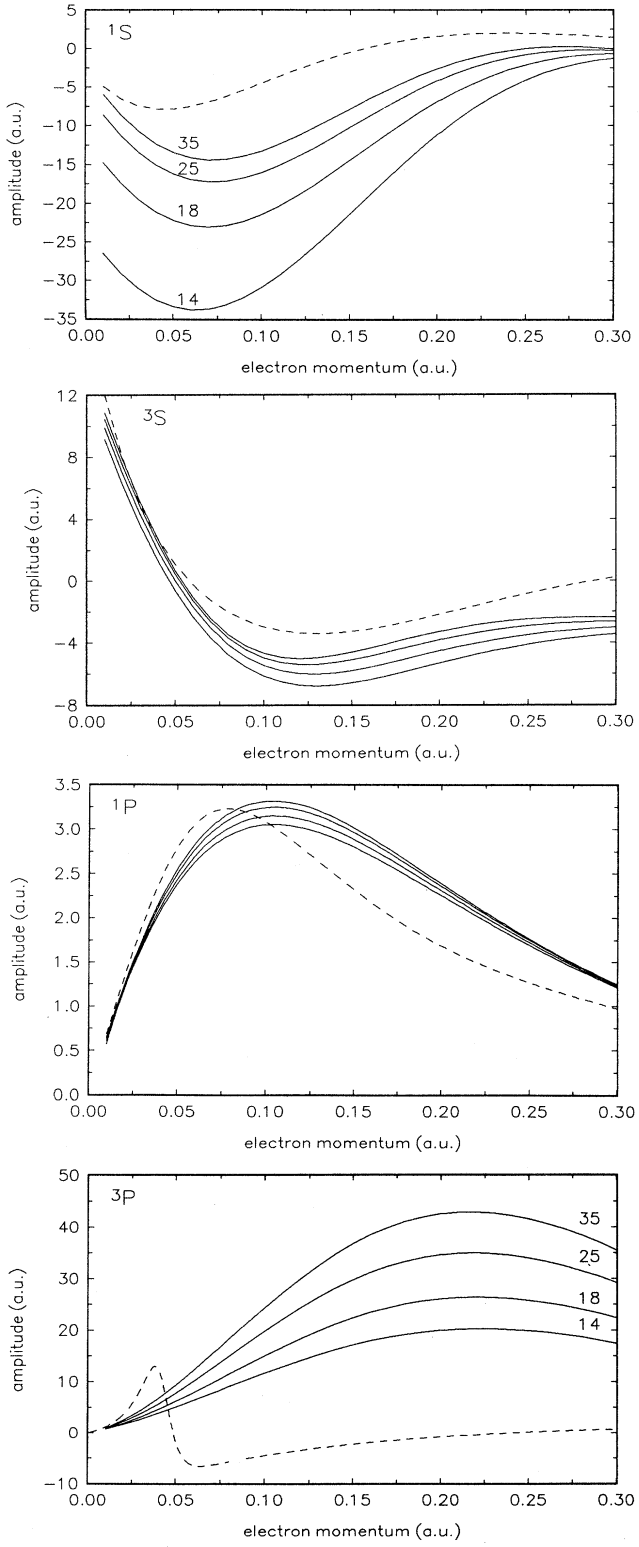

FIG. 1. Off-shell amplitudes $f(k,k,E)$ for e-Rb scattering. The energy is given by the expression $E = -1/2(n-\mu)^2$, where $\mu = 3.133$. Numbers near the curves indicate the principal quantum number n. For ^3S and ^1P scattering the values of n are the same as those for ^1S and ^3P, running from n=14 (bottom curve) to n=35 (top solid curve). Dashed curves, real parts of the on-shell amplitudes.

resonance way only as a function of energy. On the other hand, the absolute value of the amplitude is still very large and it gives the major contribution to the Rydberg collision cross section in the intermediate-n region. In Fig. 2(e) we present the off-shell e-Cs, ^3P amplitude obtained by assuming a $Cs^-(^3P)$ bound state with the energy 0.027 eV. The amplitude as a function of n passes through a pole at $n = 26.496$; therefore it has very large absolute values between $n = 20$ and $n = 35$.

Before presenting the results on inelastic scattering and broadening cross sections, we should note that the experimental data [9,10] on broadening exhibit an oscillatory dependence of the broadening rate on n in the intermediate n region (n varies between 15 and 30). We showed before [4,8] that these oscillations cannot be explained within the framework of the single-scattering (e.g., impulse) approximation, and the multiple-scattering effects, which can be taken care of by the quasimolecular approach [7], are essential for their explanation. Therefore, in this paper we will not attempt to describe the oscillations, but will try to reproduce the averaged values of the broadening rates.

In Fig. 3 we present the cross sections for the quenching of Rb(nS) states by the ground-state Rb atoms. When calculating the quenching cross sections with the off-shell amplitude we found that at $n < 14$ a substantial contribution to the cross section is given by the range of momentum $k > 0.3$. Since these momenta are too high for our amplitude to be reliable, we stopped calculations at $n = 14$. For comparison with the experiment we plot experimental data of Hugon *et al.* [26] on the destruction of Rydberg states and data of Heinke *et al.* [9] on collisional broadening. The latter have been extracted from the following relation between the broadening rate and collisional cross sections

$$\gamma/N = 2\langle V\sigma^{\rm br}(V)\rangle, \tag{30}$$

where γ is the spectral line width, N is the number density of the perturbing atoms,

$$\sigma^{\rm br} = \frac{1}{2}(\sigma^{\rm inel} + \sigma^{\rm el}) \tag{31}$$

is the broadening cross section, and the angular brackets mean the average over the velocity distribution. As we showed before [6], the approximation

$$\gamma/N \approx \langle V\rangle\sigma(\langle V\rangle) \tag{32}$$

can be used with good accuracy. Note that the difference between the broadening and the quenching rates represents the elastic-scattering contribution to the broadening, which is small for high enough n.

The difference between the on-shell (solid line) and the off-shell (dashed line) results is very large at $14 < n < 20$. The experimental points for quenching cross sections lie between the two curves in this region of n and have rather large error bars. Therefore, it is difficult to conclude which theoretical curve agrees better with the quenching experiment. The off-shell results agree better with the broadening data. However, at low n the contribution of

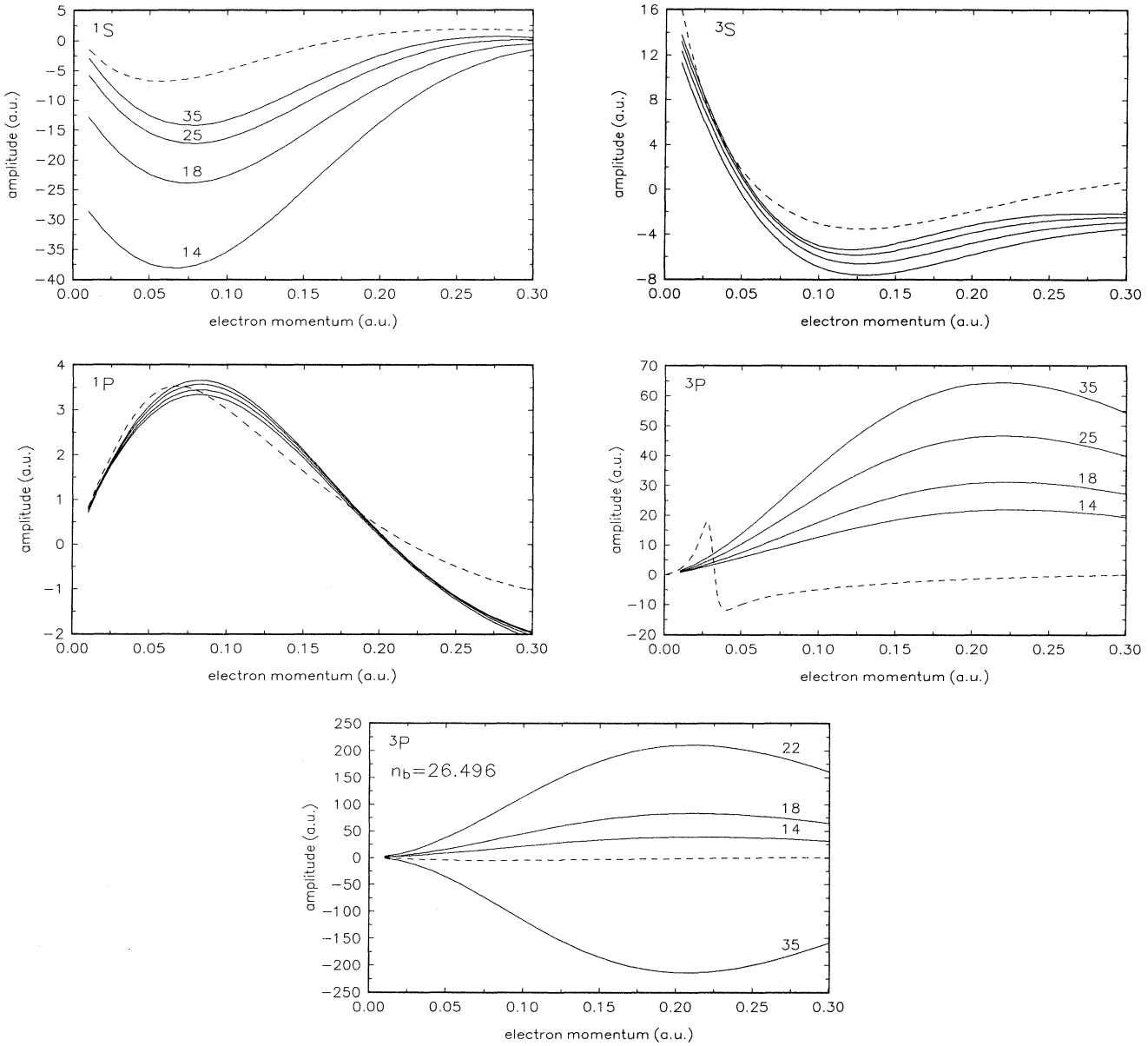

FIG. 2. Same as in Fig. 1 for e-Cs scattering, but for $\mu = 4.049$. (e) gives the ^3P amplitude in the case of the $Cs^-(^3P)$ bound state with the energy 27 meV corresponding to $n = 26.496$.

the elastic scattering to broadening might become important [6].

In Fig. 4 we present the data on quenching of the Rb(nP) states by the ground-state Rb. Once again, the difference between the two theoretical sets of results is very large at $n < 30$. It seems that the off-shell results agree better with the experiments, but, similarly to the on-shell results, they turn down sharply at $n < 17$ and become much lower than the experimental values. This indicates the importance of the multiscattering effects in the region of low n.

In Fig. 5 we present the broadening of Rb(nD) states by the ground-state Rb atoms. For a consistent comparison with the experiment we have included the contribution of the A^+-B elastic scattering, which is given by the cross section [19]

$$\sigma^{\rm el}_{A^+B} = 7.16 \left(\frac{\alpha}{v_{AB}} \right)^{2/3},$$

where α is the polarizability of the perturber. Applying this equation to Rb and Cs atoms at $T = 513$ K, we obtain 2.16×10^{-14} and 2.04×10^{-14} MHz cm^3 respectively.

The off-shell effect drastically improves the agreement with the experimental data on line broadening, although there is still some disagreement in the magnitude. We should note, however, that there are some uncertainties in the experimental data. First, there is about a factor

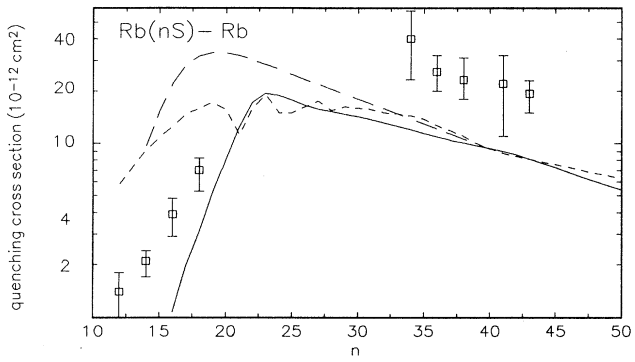

FIG. 3. Quenching cross sections for the Rb(nS)-Rb collisions. Solid curve, the on-shell calculations [6] for the collision velocity corresponding to T=530 K; long-dashed curve, the off-shell results for the same velocity; short-dashed curve, the cross sections, obtained from the broadening data [9]; squares with error bars, the experimental data [26] on the quenching cross sections.

of 2 difference between the results of Heinke *et al.* [9] and Thompson *et al.* [10]. Second, the data of Heinke *et al.* [9] are systematically slightly smaller than the previous results [28] obtained in the same experimental group. For the purpose of comparison between the two sets of experimental results Heinke *et al.* [9] suggested that one should divide the self-broadening data [10] for K by 2.08. However, the graphical results of Heinke *et al.* on the self-broadening of Rb differ from both the reduced data of Thompson *et al.* and the previous data of Weber and Niemax [28]. For the purpose of comparison with the theory we present in Fig. 5 the data of Thompson *et al.* [10] normalized to those of Heinke *et al.* at n=23.

In Fig. 6 we present the broadening rates for Cs(nS) states perturbed by the ground-state Cs. In this case both the on-shell and the off-shell results strongly exceed the experimental data up to $n = 30$. The important feature of the Cs(nS) states is a small value of the fractional part of their quantum defect. (The quantum defect $\mu = 4.049$.) The inelastic cross section in this situation is very close to that of the l-mixing process [19]. This limit treated in the scattering-length approximation gives [18]

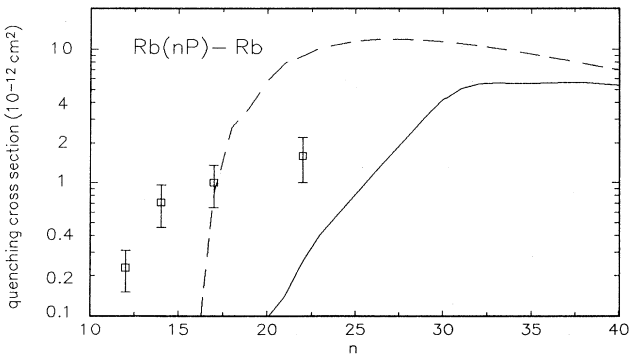

FIG. 4. Quenching cross sections for Rb(nP)-Rb collisions. Solid curve, the on-shell results [6]; dashed curve, off-shell results; squares with error bars, the experimental data [27].

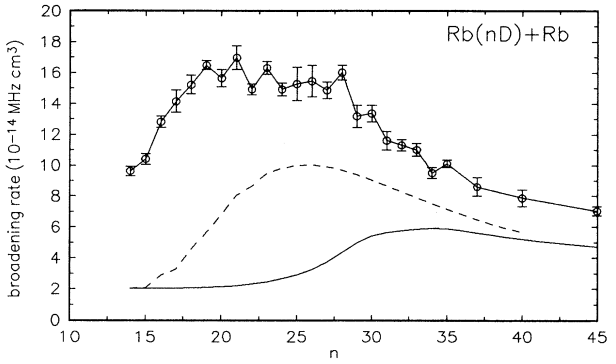

FIG. 5. Broadening of Rb(nD) states by the ground-state Rb atoms. Solid curve, the on-shell results; dashed curve, the off-shell results; circles with error bars, the experimental data [9,10] (see the text).

$$\sigma = \frac{2\pi A^2}{n^3 v_{AB}^2}. \tag{33}$$

To make an estimate in the case when the scattering-length approximation is invalid, we can replace πA^2 in the numerator of Eq. (31) by the elastic e-B scattering cross section. In any case, we obtain very large values for the alkali-metal atoms, which are much larger than the geometrical cross section $2.5\pi n^4$ of the Rydberg atom at $n < 30$. Apparently, the impulse approximation is not applicable in this case [19]. To illustrate the point, we present in Fig. 6 the "geometrical" limit of the broadening rate (dot-dashed curve), which was obtained by using the geometrical cross section for inelastic collisions. We conclude that in the region of intermediate values of n (between 20 and 30) the impulse approximation describes better quenching of those Rydberg states whose fractional part of the quantum defect is not very small. Furthermore, in this case the first-order Faddeev approximation agrees better with experiment than the standard impulse approximation.

As a further illustration of this point, we present in Fig.

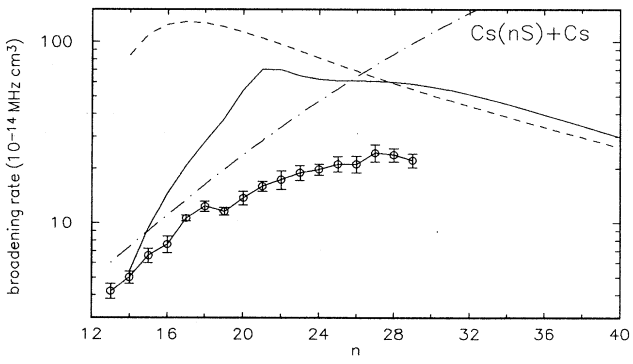

FIG. 6. Broadening of Cs(nS) states by the ground-state Cs atoms. Solid curve, the on-shell results; dashed curve, the off-shell results; dash-dotted curve, the "geometrical" limit on the cross section (see the text); circles with error bars, the experimental data [9].

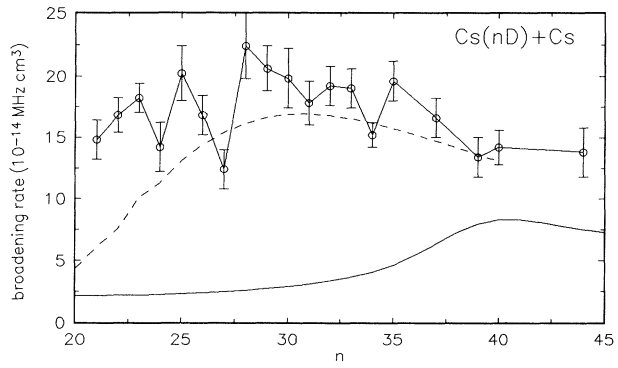

FIG. 7. Broadening of Cs(nD) states by the ground-state Cs atoms. Solid curve, the on-shell results; dashed curve, the off-shell results; circles with error bars, the experimental data [9].

7 the broadening of Cs(nD) states (quantum defect $\mu = 2.466$) perturbed by Cs atoms. Once again, the off-shell effect strongy improves agreement with the experimental data, even better than in the case of self-broadening of Rb atoms.

In Fig. 8 we present the theoretical Cs(nS)-Cs cross sections and compare them with the results obtained assuming the $Cs^-(^3P)$ bound state, corresponding to the scattering amplitude of Fig. 2(e). The cross section increases enormously and leads to strong disagreement with the experimental data. Once again, we see that experimental data on Rydberg collisions indicate the existence of a $Cs^-(^3P)$ resonance rather than a bound state, in accordance with the results of recent relativistic R-matrix calculations [29]. However, whereas in the impulse approximation the bound state leads to a reduction of the cross section, in the first-order Faddeev approximation it leads to a very large increase.

VI. CONCLUSIONS

We have demonstrated that the off-shell effects play a very important role in the Rb(nl)-Rb($5s$) and Cs(nl)-Cs($6s$) collisions at $n < 40$. We have found that the first-order Faddeev approximation reproduces the experimental results on quenching cross sections better than the standard impulse approximation. However, at low n both versions of the single-scattering approximation, that is, the impulse approximation and the first-order Faddeev approximation, become inadequate for a description of the Rydberg-atom–ground-state-atom scattering. On the other hand, at $n > 40$ off-shell and on-shell approaches give close results; therefore the off-shell effects can be neglected in this region. Typically it corresponds to the range of electron kinetic energies where the scattering length approximation is valid.

Another advantage of the first-order Faddeev amplitude is that it represents the first-order approximation to the solution of the exact three-body Faddeev equations. Higher-order corrections taking into account the multiple-scattering effect can be obtained from these equations [6] and they contain the off-shell scattering amplitude. Therefore the results obtained in the present paper serve as a basis for obtaining more precise theoretical data on the Rydberg-atom–ground-state-alkali-metal-atom collisions.

A certain interest may represent data on the Rydberg-atom collisions with the ground-state Ca atoms. The bound $Ca^-(^2P)$ state has a very small binding energy and should strongly affect these processes in the region of high n where the single-scattering approximation is more reliable. Recent experimental observatons [30] of the electron transfer in Ca(nl)-Ca($4s^2$) collisions provided a certain input for the theory [14]. An observation of the quenching of Rydberg atoms by ground-state Ca atoms would be very useful for further theoretical investigation of the off-shell effects in the Rydberg-atom–ground-state-atom scattering.

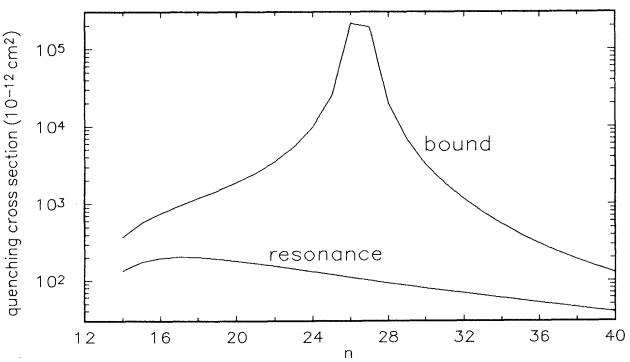

FIG. 8. Quenching cross sections for Cs(nS)-Cs collisions. The curve "resonance" corresponds to the $Cs^-(^3P)$ resonance state, the curve "bound" to the bound state with the energy 27 meV.

ACKNOWLEDGMENT

This work has been supported by the National Science Foundation through Grants No. PHY90-06612 and No. PHY92-07986.

APPENDIX A: OFF-SHELL AMPLITUDE FOR POTENTIALS WITH A HARD CORE

We apply the formulas for the off-shell amplitude to a particular case when the potential has a hard core

$$V(r) = \begin{cases} U_0 = \infty & \text{when } r < a \\ U(r) & \text{when } r > a. \end{cases} \quad \text{(A1)}$$

First, we will obtain the expressions with a finite U_0 and then make it infinite.

In this appendix it will be convenient to use Riccati-Bessel functions (see Appendix B) and to introduce the parameters

$$\chi = \sqrt{2E}, \quad \text{(A2)}$$

$$\gamma = \sqrt{2(V(r) - E)}. \quad \text{(A3)}$$

Equation (25) now becomes

$$\left(\frac{d^2}{dr^2}-\gamma^2-\frac{l(l+1)}{r^2}\right)u_l(kr,E)=\frac{\gamma^2+\chi^2}{2k}\mathcal{J}_l(kr), \tag{A4}$$

where $\mathcal{J}_l(kr)$ is the Riccati-Bessel function.

1. Calculation of $u_l(kr)$

The solution of Eq. (A4) is

$$u_l(kr,E)=\begin{cases} B\mathcal{J}_l(kr)+A\mathcal{J}_l(i\gamma r) & \text{for } r<a \\ g_l(r)+Cf_l(r) & \text{for } r>a, \end{cases} \tag{A5}$$

where the first terms are partial solutions of the inhomogeneous equation and the second ones are the general solutions of the homogeneous equation. The coefficient B is uniquely determined by the differential equation and, using Eq. (B1) (see Appendix B) for the Riccati-Bessel functions, can be shown to be

$$B=-\frac{1}{2k}\frac{\gamma^2+\chi^2}{\gamma^2+k^2}. \tag{A6}$$

The coefficients A and C should be found by matching the solutions at $r=a$

$$A\mathcal{J}_l(i\gamma a)-Cf_l(a)=g_l(a)-B\mathcal{J}_l(ka), \tag{A7}$$

$$A\frac{d\mathcal{J}_l(i\gamma a)}{da}-C\frac{df_l(a)}{da}=g_l'(a)-B\frac{\mathcal{J}_l(ka)}{da}. \tag{A8}$$

Solving these equations, we obtain for the coefficients A and C

$$A=\frac{\mathcal{W}(f_l(a),g_l(a)-B\mathcal{J}_l(ka))}{\mathcal{W}(f_l(a),\mathcal{J}_l(i\gamma a))}, \tag{A9}$$

$$C=\frac{\mathcal{W}(-g_l(a)+B\mathcal{J}_l(ka),\mathcal{J}_l(i\gamma a))}{\mathcal{W}(f_l(a),\mathcal{J}_l(i\gamma a))}, \tag{A10}$$

where $\mathcal{W}$ is a Wronskian defined by Eq. (B10) (see Appendix B). The limits of the coefficients as $\gamma\to\infty$ are

$$B_\infty=-\frac{1}{2k}, \tag{A11}$$

$$A_\infty=\frac{2\exp(-\gamma a)}{i^{l+1}\gamma}\frac{\mathcal{W}(f_l(a),g_l(a)+\frac{1}{2k}\mathcal{J}_l(ka))}{f_l(a)}, \tag{A12}$$

$$C_\infty=-\frac{g_l(a)+\frac{1}{2k}\mathcal{J}_l(ka)}{f_l(a)}. \tag{A13}$$

2. Contributions to the amplitude from the core ($r<a$)

Equation (22) immediately gives

$$f_{l<}^{(1)}(k',k)=-\frac{\gamma^2+\chi^2}{k'k}\int_0^a\mathcal{J}_l(k'r)\mathcal{J}_l(kr)\,dr. \tag{A14}$$

When evaluating Eq. (23), we distinguish between the contributions from inhomogeneous and homogeneous solutions

$$f_{l<}^{(2i)}(k',k)=\frac{(\gamma^2+\chi^2)^2}{k'k(\gamma^2+k^2)}\int_0^a\mathcal{J}_l(k'r)\mathcal{J}_l(kr)\,dr, \tag{A15}$$

$$f_{l<}^{(2h)}(k',k)=-\frac{2A(\gamma^2+\chi^2)}{k'}\int_0^a\mathcal{J}_l(k'r)\mathcal{J}_l(i\gamma r)\,dr, \tag{A16}$$

where the relevant integrals are calculated in Appendix B [see Eqs. (B12) and (B13)]. To obtain the limiting forms we combine Eqs. (A14) and (A15) together and use Eqs. (A12) and (B13) in Eq. (A16):

$$\begin{aligned} f_{l<}^{(1)}(k',k)+f_{l<}^{(2i)}(k',k) &= \frac{(\gamma^2+\chi^2)(\chi^2-k^2)}{k'k(\gamma^2+k^2)}\int_0^a\mathcal{J}_l(k'r)\mathcal{J}_l(kr)\,dr \\ &\xrightarrow{\gamma\to\infty}\frac{\chi^2-k^2}{k'k}\int_0^a\mathcal{J}_l(k'r)\mathcal{J}_l(kr)\,dr, \end{aligned} \tag{A17}$$

$$f_{l<}^{(2h)}(k',k)\xrightarrow{\gamma\to\infty}-2\mathcal{J}_l(k'a)\frac{\mathcal{W}(f_l(a),g_l(a)+\frac{1}{2k}\mathcal{J}_l(ka))}{k'f_l(a)}. \tag{A18}$$

3. Contribution from the region $r>a$

From Eqs. (22) and (23) we obtain

$$f_{l>}^{(1)}(k',k)=-\frac{2}{k'k}\int_a^\infty U(r)\mathcal{J}_l(k'r)\mathcal{J}_l(kr)\,dr, \tag{A19}$$

$$f_{l>}^{(2)}(k',k)=-\frac{4}{k'}\int_a^\infty U(r)\mathcal{J}_l(k'r)[g_l(r)+C_\infty f_l(r)]\,dr \quad \text{as } \gamma\to\infty, \tag{A20}$$

where C_∞ is given by Eq. (A13). The final result for the off-shell amplitude for the potentials with a hard core is the sum of Eqs. (A17), (A18), (A19), and (A20).

It is interesting to consider the scattering amplitude *on shell* for the hard sphere, i.e., $k=k'=\chi$ and $U(r)=0$ $\forall r>a$. In this case $g_l(r)=0$ and $f_l(r)=\mathcal{H}_l(\chi r)$. Only Eq. (A18) gives a nonzero contribution and, using the Wronskian (B11), we obtain the expected result for the amplitude

$$f_l(\chi)=\frac{i\mathcal{J}(\chi a)}{\chi\mathcal{H}_l^{(1)}(\chi a)}. \tag{A21}$$

APPENDIX B: EXPRESSIONS WITH RICCATI-BESSEL FUNCTIONS USED IN THIS PAPER

1. Differential equation and linearly independent solutions

The differential equation for the Riccati-Bessel functions is

$$\frac{d^2}{dr^2}W_l(kr) + \left(k^2 - \frac{l(l+1)}{r^2}\right) W_l(kr) = 0 \qquad \text{(B1)}$$

and the linearly independent solutions are

$$\mathcal{J}_l(kr) = krj_l(kr), \qquad \text{(B2)}$$

$$\mathcal{N}_l(kr) = kr\eta_l(kr), \qquad \text{(B3)}$$

$$\mathcal{H}_l^{(1,2)}(kr) = krh_l^{(1,2)}(kr), \qquad \text{(B4)}$$

where j_l, η_l, and $h_l^{(1,2)}$ are the spherical Bessel functions.

2. Recurrence relations

The recurrence relations follow directly from those for spherical Bessel functions [31]

$$W_{l+1}(z) = \frac{2l+1}{z}W_l(z) - W_{l-1}(z), \qquad \text{(B5)}$$

$$\frac{dW_l}{dz} = W_{l-1}(z) - \frac{l}{z}W_l(z), \qquad \text{(B6)}$$

$$\frac{dW_l}{dz} = \frac{l+1}{z}W_l(z) - W_{l+1}(z). \qquad \text{(B7)}$$

3. Asymptotic behavior

We need only one function $\mathcal{J}_l$ and here is its asymptotic behavior for large imaginary argument

$$\mathcal{J}_l(ix) \to \frac{i^{l+1}}{2}\exp(x) \text{ as } x \to \infty, \qquad \text{(B8)}$$

$$\mathcal{J}_l'(ix) \to \frac{i^l}{2}\exp(x) \text{ as } x \to \infty. \qquad \text{(B9)}$$

4. Wronskians

We define the Wronskian as

$$\mathcal{W}(W(kx), V(kx)) = W\frac{dV}{dx} - V\frac{dW}{dx}. \qquad \text{(B10)}$$

With this definition, we have

$$\mathcal{W}(\mathcal{J}_l(kx), \mathcal{H}_l^{(1)}(kx)) = ik. \qquad \text{(B11)}$$

5. Important integrals

Using the differential equation (B1) for Riccati-Bessel functions it is not difficult to show that

$$\int_0^a \mathcal{J}_l(k'r)\mathcal{J}_l(kr)\,dr = \frac{\mathcal{W}(\mathcal{J}_l(k'a), \mathcal{J}_l(ka))}{k'^2 - k^2}, \qquad \text{(B12)}$$

where the Wronskian is defined by Eq. (B10). The asymptotic form (B9) gives the limit of the above integral for large purely imaginary $k = i\gamma$:

$$\int_0^a \mathcal{J}_l(k'r)\mathcal{J}_l(i\gamma r)\,dr \to \frac{i^{l+1}}{2\gamma}\exp(\gamma a)\mathcal{J}_l(k'a) \text{ as } \gamma \to \infty. \qquad \text{(B13)}$$

Another important case is $k' = k$. The $\frac{0}{0}$ uncertainty in Eq. (B12) can be resolved by l'Hospital's rule and we get

$$\int_0^a \mathcal{J}_l^2(kr)\,dr = \frac{a}{2}\left[\mathcal{J}_l^2(ka) + \mathcal{J}_{l-1}^2(ka)\right] - \frac{l+1/2}{k}\mathcal{J}_l(ka)\mathcal{J}_{l-1}(ka). \qquad \text{(B14)}$$

[1] E. Fermi, Nuovo Cimento **11**, 157 (1934).

[2] M. Matsuzawa, in *Rydberg States of Atoms and Molecules*, edited by R.F. Stebbings and F.B. Dunning (Cambridge University Press, Cambridge, 1983), p. 267.

[3] M. Kimura, R.E. Olson, and J. Pascale, Phys. Rev. A **26**, 3113 (1982); A. Kumar, N.F. Lane, and M. Kimura, *ibid.* **39**, 1020 (1989).

[4] V.M. Borodin, I.I. Fabrikant, and A.K. Kazansky, Phys. Rev. A **44**, 5725 (1991).

[5] M.R. Flannery, in *Rydberg States of Atoms and Molecules* (Ref. [2]), p. 393.

[6] I.I. Fabrikant, Phys. Rev. A **45**, 6404 (1992).

[7] V.M. Borodin and A.K. Kazansky, J. Phys. B **25**, 971 (1992).

[8] V.M. Borodin, A.K. Kazansky, D.B. Khrebtukov, and I.I. Fabrikant, Phys. Rev. A **48**, 479 (1993).

[9] H. Heinke, J. Lawrentz, K. Niemax, and K.-H. Weber, Z. Phys. A **312**, 329 (1983).

[10] D.C. Thompson, E. Weinberger, G.-X. Xu, and B.P. Stoicheff, Phys. Rev. A **35**, 690 (1987); B.P. Stoicheff and E. Weinberger, Phys. Rev. Lett. **44**, 733 (1980).

[11] L.D. Faddeev, Zh. Eksp. Teor. Fiz. **39**, 1459 (1960) [Sov. Phys. JETP **12**, 1014 (1961)]; more details about the Faddeev equations could be found in the book of E.W. Schmid and H. Ziegelmann, *The Quantum Mechanical Three-Body Problem* (Pergamon, Oxford, 1974).

[12] J.C.Y. Chen and T. Ishihara, Phys. Rev. **186**, 25 (1969); P.J. Kramer and J.C.Y. Chen, Phys. Rev. A **3**, 568 (1971).

[13] E. de Prunelé, Phys. Rev. A **27**, 1831 (1983).

[14] I.I. Fabrikant, Phys. Rev. A **48**, R3411 (1993).

[15] M. Matsuzawa, J. Phys. B **10**, 1543 (1977).

[16] I.I. Fabrikant, J. Phys. B **19**, 1527 (1986).

[17] V.A. Alekseev and I.I. Sobel'man, Zh. Eksp. Teor. Fiz. **49**, 1274 (1965) [Sov. Phys. JETP **22**, 882 (1966)].

[18] A. Omont, J. Phys. (Paris) **38**, 1343 (1977).

[19] V.S. Lebedev and V.S. Marchenko, J. Phys. B **20**, 6041 (1987); Zh. Eksp. Teor. Fiz. **91**, 428 (1986) [Sov. Phys. JETP **64**, 251 (1986)].

[20] I.M. Gel'fand and B.M. Levitan, Izv. Akad. Nauk SSSR **15**, 309 (1951) [Am. Math. Soc. Transl. **1**, 253 (1955)]; more details about the inverse problem could be found in the book of R.G. Newton, *Inverse Schrödinger Problem in Three Dimensions* (Springer-Verlag, Berlin, 1989).

[21] J. Pascale, Phys. Rev. A **28**, 632 (1983).

[22] M.L. Goldberger and K.M. Watson, *Collision Theory*

(Wiley, New York, 1964), Sec. 5.3.
[23] J.E. Dennis, Jr. and D.J. Woods, *New Computing Environments: Microcomputers in Large-Scale Computing*, edited by A. Wouk (Society for Industrial and Applied Mathematics, Philadelphia, 1987), pp. 116–122.
[24] I.I. Fabrikant, Opt. Spektrosk. **53**, 223 (1982) [Opt. Spectrosc. (USSR) **53**, 131 (1982)].
[25] D.B. Khrebtukov, J. Phys. A **26**, 6357 (1993).
[26] M. Hugon, F. Gounand, and P.R. Fournier, J. Phys. B **13**, L109 (1980); M. Hugon, F. Gounand, P.R. Fournier, and J. Berlande, *ibid.* **16**, 2531 (1983).
[27] F. Gounand, P.R. Fournier, and J. Berlande, Phys. Rev. A **15**, 2212 (1977).
[28] K.-H. Weber and K. Niemax, Opt. Commun. **28**, 317 (1979); **31**, 52 (1979).
[29] U. Thumm and D.W. Norcross, Phys. Rev. Lett. **67**, 3495 (1991).
[30] K.W. McLaughlin and D.W. Duquette, Phys. Rev. Lett. **72**, 1176 (1994).
[31] *Handbook of Mathematical Formulas*, edited by M. Abramowitz and I. Stegun (Dover, New York, 1972), p. 437.